Structural Transition Behavior of Potassium Salts of Saturated Fatty Acids, $CH_3(CH_2)_nCO_2K$ (n=14, 16, 18, 20)

Tsutomu ISHIOKA
Department of Material Systems Engineering, Faculty of Technology,
Tokyo University of Agriculture and Technology, Koganei, Tokyo 184
(Received January 16, 1991)

The structural transition behavior of potassium soaps (99% purity), $CH_3(CH_2)_nCO_2K$ (n=14, 16, 18, 20), having low water contents of less than 10 wt% was investigated by both DSC and vibrational spectroscopies. Nine phases from crystal (I<80 °C) to liquid crystal (260 °C<IX) were observed for n=14 and 16 by thermal measurements. An additional phase I′ (I<I′<II) was found for n=18 and 20. The structural changes of the alkyl chains accompanied by these transitions were investigated by using IR and Raman methods. With increase in temperature, the itensities of the IR methylene progressive bands which were characteristic of all-trans conformation decreased and conformational defect bands ascribed to *gt*-, *gg*-, and *gtg′* conformations, were observed in phases I′, II, and III for n=14—20. These indicate the onset of a partial melting of the chains in these phases. At the transition from phase III to IV, the chains entered liquid-like conformations. The result was also confirmed by the Raman spectra.

Even-numbered anhydrous potassium soaps, $CH_3(CH_2)_nCO_2K$ (where n is the number of the methylene groups), take successive phase transitions from the crystalline phase to the liquid crystalline phase with an increase in temperature.[1] The lowest temperature crystalline phase of n=10—16 is ascribed to the triclinic B-form (space group $P\bar{1}$). The unit cell contains two molecules having an all-trans conformation. The molecules are parallel to each other and are packed with a triclinic $T_{//}$ subcell. With an elevation in temperature, the B-form is transformed to the monoclinic C-form ($P2_1/a$) at 50—80 °C. The molecule in the C-form is supposed to have a partially conformational disorder at the methyl end. A further increase in the temperature causes the transition from the crystalline phase to the two-dimensional rectangular or oblique lattice at 170—195 °C for n=12—16. The lattice is changed into the lamellar liquid crystalline phase at 270—280 °C.

Several experimental techniques, such as x-ray diffraction or NMR methods, have been applied in order to characterize the molecular structure in these phases, while the detailed molecular transition behavior, especially the melting process of the alkyl chains during these successive transitions, has not yet been clearly shown. In this study, we tried to clarify the melting behavior of the alkyl chains in soaps with n=14, 16, 18, and 20 using differential scanning calorimetry (DSC), infrared, and Raman methods.

Experimental

Potassium soaps of n=14—20 were synthesized from even-numbered saturated fatty acids (Σ company, 99%) by the titration of potassium carbonate in ethanol solution kept at 70 °C. The products were purified by reprecipitation with diethyl ether from the solutions and dried at 100 °C in vacuo for 24 h. Neutralization was confirmed by the IR spectrum. The contents of water were evaluated as a few wt% by a elementary analysis.

DSC measurements were carried out with a Rigaku DSC using sealed pans at a heating rate 10 K min^{-1}. The transition temperatures and enthalpy changes were calibrated using seven standards: carbon tetrachloride, benzene, naphthalene, benzoic acid, indium, tin, and lead. Infrared measurement was made with a JASCO IR-810 spectrophotometer. The wavenumbers were calibrated with an indene standard. The sample for IR measurements was pressed into a KBr disk. Raman measurements were made with a JASCO R-800 double monochromator using a 514.5 nm exciting beam from an Ar^+ laser. A powder sample sealed in a glass capillary was subjected to a Raman measurement. The heating rate for the IR and Raman measurements was 10 K min^{-1}. In order to achieve thermal equilibrium, the measurements were carried out after 1 h of temperature setting.

Results and Discussion

The results of DSC measurements for n=14, 16, 18, and 20 are shown in Fig. 1. With increasing temperature from room temperature to 280 °C, eight endothermic peaks were observed for n=14 and 16 and nine peaks for n=18 and 20. According to Cingolani et al.,[2] these transitions are described with symbols from b′ to F, as shown in Fig. 1. Their temperatures, enthalpy, and entropy changes were the same as those obtained by Cingolani et al.[2] for n=14, 16, and 18 within the experimental error. Those for n=20 are listed in Table 1. Nine phases were designated as from phase I

Table 1. Transition Temperatures, Enthalpy, and Entropy Changes for n=20

	t	ΔH	ΔS
	K	kJ mol^{-1}	J K^{-1} mol^{-1}
I→I′	342.0	2.5	7.2
I′→II	361.1	14.9	41.2
II→III	403.2	1.8	4.5
III→IV	427.7	2.3	5.4
IV→V	450.2	12.3	27.2
V→VI	488.8	0.5	1.1
VI→VII	501.3	0.6	1.2
VII→VIII	519.4	1.0	1.9
VIII→IX	538.6	9.4	17.5

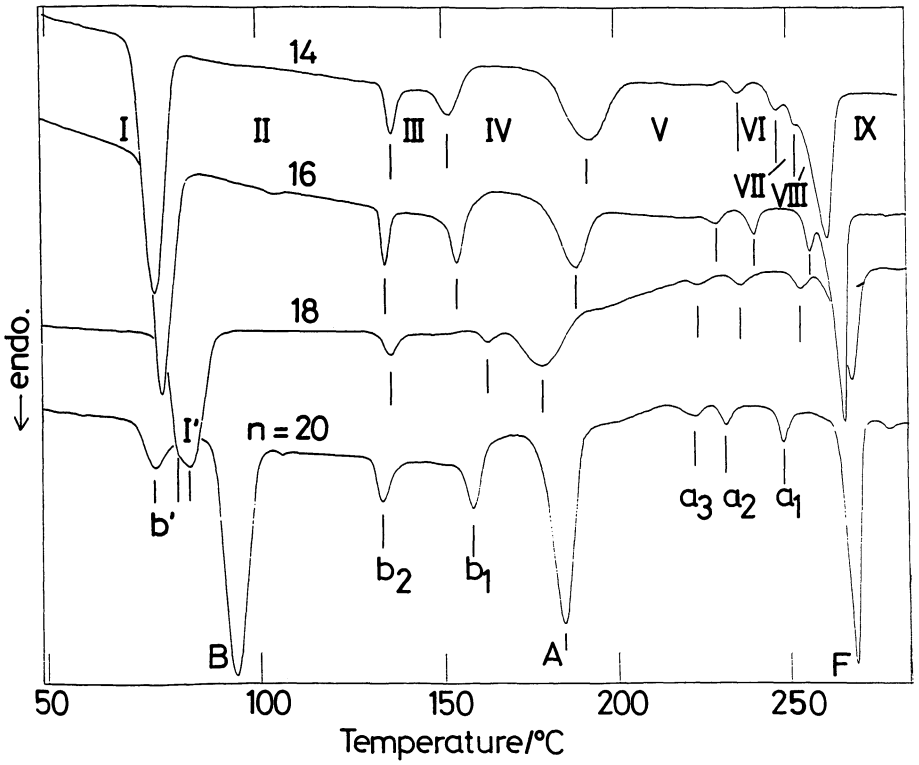

Fig. 1. DSC curves for n=14—20.

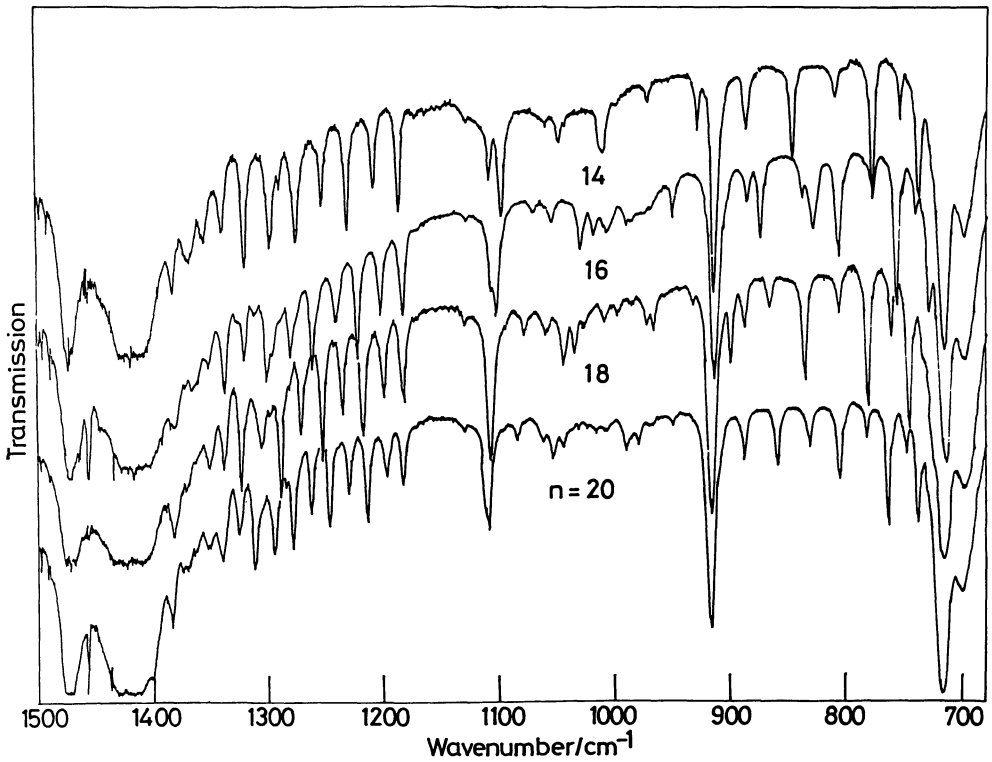

Fig. 2. IR spectra for n=14—20 in the 700—1400 cm^{-1} region at room temperature.

Table 2. Observed and Calculated Frequencies (cm^{-1}) for $n=14$

ν_{obsd}	Relative intensity[a)]	ν_{calcd}	P. E. D. (%)[b)]			
A′ mode						
1417	s	1414	δ(44),	W(22),	R(15),	ν_s(COO)(14)
		1410	W(54),	R(30),	δ(13)	
		1404	W(60),	R(30)		
		1394	W(60),	R(27),	δ(11)	
1385	m	1383	W(61),	R(25),	δ(10)	
		1373	U(70),	W(15),	R(11)	
1367	m	1367	W(59),	R(17),	U(16)	
1357	m	1351	W(73),	R(16)		
1340	m	1332	W(80),	R(11)		
1322	m	1312	W(86)			
1299	m	1294	W(89)			
1276	m	1276	W(87)			
1253	m	1257	W(83)			
1232	m	1235	W(78),	ω(11)		
1209	m	1208	W(76),	ω(10)		
1188	m	1181	W(83)			
1130	w	1129	R(39),	ω(33),	W(13)	
1099	m	1093	R(41),	ω(27),	W(21)	
		1069	R(81),	W(17)		
		1067	R(78),	W(15)		
		1065	R(76),	W(17)		
1061	w	1061	R(82),	W(17)		
		1058	R(80),	W(17)		
		1054	R(82),	W(11)		
1049	w	1050	R(66),	W(15),	ω(15)	
		1033	R(75),	W(10),	ω(10)	
1014	m	1017	R(80),	W(10)		
998	vw	1000	R(72),	ω(13)		
		983	R(80),	ω(11)		
		973	R(78),	ω(12)		
917	m	891	R(47),	β(33)		
889	m	888	R(49),	δ(COO)(39)		
A″ mode						
		1302	T(96)			
		1302	T(97)			
		1300	T(98)			
		1299	T(95)			
		1297	T(97)			
		1296	T(100)			
		1294	T(90)			
1289	w	1286	T(85),	P(12)		
		1274	T(79),	P(17)		
1258	vw, sh	1259	T(72),	P(23)		
		1241	T(62),	P(32)		
		1219	T(49),	P(43)		
		1196	P(59),	T(30)		
1174	vw	1177	P(82)			
1109	m	1103	T(64),	P(32)		
1043	vw, sh	1036	T(88),	P(10)		
1011	m	1005	T(70),	P(24)		
973	w	968	T(56),	P(35)		
931	m	930	P(45),	T(45)		
889	m	890	P(54),	T(36)		
849	m	851	P(62),	T(28)		
812	w	813	P(69),	T(21)		
779	m	778	P(76),	T(15)		
755	m	745	P(82),	T(11)		
739	m	718	P(88)			
727	w, sh	695	P(92)			
		679	P(96)			
		667	P(98)			
716	s	661	P(100)			

a) s, m, w, v, sh mean strong, medium, weak, very, and shoulder. b) P. E. D.=potential energy distribution where W, R, P, T, U, β, ω, δ, ν_s(COO), and δ(COO) indicate methylene wagging, C–C stretching, methylene rocking-twisting, twisting-rocking, methyl symmetric bending, rocking, C–C–C bending, methylene bending, carboxylate symmetric stretching, and bending, respectively.

Table 3. Observed and Calculated Frequencies (cm^{-1}) for n=16

ν_{obsd}	Relative intensity	ν_{calcd}	P. E. D. (%)			
A′ mode						
		1416	W(45),	R(27),	δ(17)	
1419	s	1413	W(40),	δ(28),	R(23)	
		1408	W(53),	R(28),	δ(16)	
		1401	W(57),	R(28),	δ(13)	
		1391	W(60),	R(26),	δ(11)	
1385	w	1380	W(60),	R(23)		
1371	vw, sh	1372	U(77),	W(11)		
1364	w	1364	W(66),	R(18)		
1355	w	1348	W(75),	R(15)		
1340	m	1331	W(81),	R(10)		
1323	m	1314	W(86),			
1303	m	1298	W(88)			
1283	m	1282	W(88)			
1263	m	1266	W(86)			
1244	m	1245	W(82),	ω(10)		
1224	m	1227	W(78),	ω(11)		
1205	m	1203	W(77),	ω(10)		
1185	m	1178	W(86)			
1130	w	1127	R(39),	ω(34),	W(11),	β(10)
1104	m	1096	R(40),	ω(28),	W(20)	
1072	w	1072	R(74),	W(18)		
		1071	R(80),	W(18)		
		1069	R(74),	W(20)		
		1066	R(81),	W(17)		
		1063	R(76),	W(16)		
		1062	R(75),	W(17)		
1056	w	1061	R(78),	W(16)		
		1048	R(69),	ω(13),	W(13)	
1030	w	1037	R(78),	W(10)		
		1019	R(84)			
1003	vw	1009	R(65),	ω(17),	W(13)	
991	w	992	R(82)			
		975	R(73),	ω(15),	W(10)	
970	vw	969	R(80),	ω(11)		
917	m	890	R(48),	β(32)		
888	w	888	R(48),	δ(COO)(40)		
A″ mode						
		1302	T(92)			
		1302	T(96)			
		1300	T(97)			
		1300	T(96)			
		1298	T(95)			
1297	m, sh	1297	T(99)			
		1296	T(100)			
1291	w	1294	T(90)			
		1287	T(86),	P(12)		
1280	w, sh	1278	T(81),	P(16)		
		1265	T(75),	P(22)		
1259	w, sh	1250	T(67),	P(28)		
		1232	T(57),	P(37)		
1219	vw, sh	1212	P(49),	T(43)		
		1192	P(64),	T(25)		
1173	vw	1176	P(85)			
		1102	T(64),	P(32)		
1042	vw	1039	T(90),			
1020	w	1014	T(75),	P(21)		
987	w	982	T(62),	P(32)		
951	w	948	T(51),	P(41)		
914	vw, sh	914	P(49),	T(41)		
877	m	879	P(57),	T(34)		
841	m	844	P(64),	T(27)		
809	m	811	P(70),	T(21)		
780	m	779	P(76),	T(16)		
759	m	750	P(82),	T(12)		
743	m	725	P(87)			
732	m	704	P(91)			
		687	P(94)			
		674	P(97)			
		665	P(99)			
716	s	660	P(100)			

(crystalline phase) to phase IX (lamellar liquid crystalline phase) for n=14 and 16. An additional phase I′ was observed for n=18 and 20. The crystal structure of phase I of n=14—20 was ascribed to the triclinic B-form by analysis of the X-ray powder pattern, while that of phase I′ of n=18 and 20 is uncertain at the present stage. Transition A was attributed to that from the crystalline phase to the two-dimensional lattice and F from the lattice to the lamellar liquid-crystalline phase.

In order to reveal any structural changes in the alkyl chains accompanied by these transitions, the temperature dependence of the IR and Raman spectra was measured. First, the spectra of n=14—20 at room temperature (phase I) were measured (Fig. 2) and their assignments were made with a normal coordinate calculation. The calculation was carried out by the Wilson GF matrix method using an NEC computer (ACOS 1000) at this university. The molecules were assumed to have an all-trans conformation and to belong to the C_s point group. A tetrahedral geometry was assumed for C–C–C, C–C–H, and H–C–H angles with C–C and C–H bond lengths equal to 1.54 and 1.093 Å, respectively. The C–C–O and O–C–O angles were assumed to be 120° with a C–O length equal to 1.27 Å.[3] The force constants regarding $CH_3(CH_2)_n$ group were transformed from the valence force constants derived by Snyder for normal paraffins (calculation V).[4] For the constants of the $C_\alpha H_2$ group and the torsional constants around all of the C–C bonds, those derived by Umemura were used.[5] For the COO^- group, the Urey-Bradley force constants derived by Nakamura[3] were transformed into the valence force constants[6] as initial values, and then adjusted to fit both

Table 4. Observed and Calculated Frequencies (cm^{-1}) for n=18

A′ mode						A″ mode				
ν_{obsd}	Relative intensity	ν_{calcd}	P. E. D. (%)			ν_{obsd}	Relative intensity	ν_{calcd}	P. E. D. (%)	
1417	s	1414	δ(49),	W(18),	R(13)			1302	T(96)	
		1410	W(61),	R(33)				1302	T(96)	
		1406	W(59),	R(31)				1301	T(96)	
		1400	W(60),	R(29),	δ(10)	1300	w	1300	T(97)	
		1393	W(61),	R(27),	δ(10)			1298	T(98)	
		1384	W(62),	R(25)				1298	T(95)	
1385	m	1374	W(41),	U(34),	R(18)			1297	T(98)	
1373	w	1371	U(50),	W(33),	R(12)			1296	T(99)	
		1360	W(70),	R(18)				1294	T(90)	
1352	w	1346	W(76),	R(14)		1283	vw, sh	1288	T(86),	P(12)
1340	m	1331	W(81),	R(10)				1280	T(81),	P(16)
1324	m	1315	W(86)					1270	T(76),	P(20)
1307	m	1301	W(88)					1257	T(70),	P(26)
1289	m	1287	W(89)					1242	T(62),	P(33)
1272	m	1272	W(87)					1225	T(52),	P(41)
1253	m	1257	W(83)					1206	P(53),	T(39)
1236	m	1240	W(79),	ω(11)				1188	P(69),	T(22)
1219	m	1221	W(76),	ω(12)		1172	vw	1176	P(87)	
1201	m	1199	W(76),	ω(11)		1095	vw	1103	T(64),	P(32)
1185	m	1176	W(86)			1044	w	1041	T(92)	
1131	w	1131	R(40),	ω(35),	W(10)			1020	T(78),	P(18)
1108	m	1104	R(39),	ω(29),	W(21)			993	T(66),	P(29)
1078	w	1074	R(50),	ω(21),	W(21)	967	w	963	T(56),	P(38)
		1067	R(81),	W(16)		933	vw	932	T(47),	P(46)
		1067	R(79),	W(17)		900	m	901	P(53),	T(39)
		1065	R(80),	W(16)		868	w	870	P(59),	T(32)
1060	w	1063	R(82),	W(17)		836	m	839	P(65),	T(26)
		1059	R(82),	W(17)		807	w	809	P(71),	T(21)
		1057	R(78),	W(16)		781	m	780	P(77),	T(16)
		1056	R(79),	W(15)		761	m	754	P(82),	T(12)
		1054	R(81),	W(11)		746	m	731	P(86)	
1035	w	1037	R(84)			735	w, sh	711	P(90)	
1026	vw	1031	R(61),	ω(18),	W(16)	726	m, sh	694	P(93)	
1009	w	1015	R(85)					681	P(96)	
998	w	1000	R(69),	ω(16),	W(11)			671	P(97)	
986	vw	991	R(81)					664	P(99)	
		974	R(77),	ω(13)		716	s	660	P(100)	
972	w	971	R(80),	ω(12)						
917	m	891	R(47),	β(33)						
888	w	888	R(49),	δ(COO)(40)						

Table 5. Observed and Calculated Frequencies (cm^{-1}) for n=20

ν_{obsd}	Relative intensity	ν_{calcd}	P. E. D. %)			
A′ mode						
1420	s	1414	δ(49),	W(18),	ν_s(COO)(15),	R(13)
		1411	W(61),	R(34)		
		1407	W(60),	R(32)		
		1403	W(60),	R(30)		
		1396	W(60),	R(28)		
		1389	W(62),	R(26)		
1385	vw	1380	W(60),	R(24)		
1372	vw	1373	U(58),	W(25),	R(13)	
		1368	W(54),	U(22),	R(16)	
1362	vw	1357	W(71),	R(17)		
1352	w	1344	W(76),	R(14)		
1340	w	1330	W(82),	R(10)		
1326	w	1316	W(86)			
1311	m	1303	W(88)			
1293	m	1290	W(89)			
1277	m	1278	W(88)			
1261	m	1265	W(85)			
1246	m	1250	W(82),	ω(10)		
1229	m	1234	W(78),	ω(11)		
1214	m	1216	W(76),	ω(12)		
1197	m	1195	W(76),	ω(10)		
1183	m	1175	W(87)			
1130	w	1131	R(41),	ω(36)		
1111	m, sh	1107	R(39),	ω(30),	W(21)	
		1079	R(46),	ω(24),	W(22)	
		1068	R(80),	W(16)		
		1068	R(81),	W(17)		
		1065	R(80),	W(17)		
		1064	R(78),	W(16)		
1063	w	1062	R(80),	W(13)		
		1061	R(80),	W(16)		
		1058	R(81),	W(17)		
1054	w	1056	R(83),	W(17)		
		1050	R(84)			
1045	w	1045	R(64),	ω(16),	W(15)	
1031	vw	1033	R(75),	ω(10),	W(10)	
1026	vw	1021	R(81)			
1008	vw	1009	R(67),	ω(15),	W(12)	
		996	R(83)			
980	w	986	R(73),	ω(14)		
		973	R(81),	ω(11)		
968	vw	969	R(78),	ω(12)		
917	m	889	R(49),	β(31)		
888	m	888	R(49),	δ(COO)(40)		
A″ mode						
		1303	T(95)			
1305	w	1302	T(96)			
		1302	T(95)			
		1301	T(96)			
		1300	T(97)			
		1299	T(95)			
		1298	T(96)			
		1297	T(99)			
		1296	T(100)			
		1294	T(89),	P(10)		
		1289	T(85),	P(13)		
1284	w	1281	T(81),	P(17)		
		1271	T(77),	P(21)		
		1259	T(71),	P(27)		
		1246	T(65),	P(33)		
		1230	T(56),	P(42)		
		1212	P(53),	T(46)		

Table 5. (Continued)

ν_{obsd}	Relative intensity	ν_{calcd}	P. E. D. %)		
		1194	P(67),	T(31)	
		1179	P(86),	T(12)	
1108	m	1103	T(64),	P(32)	
1184	w	1086	T(75),	P(24)	
1037	vw	1040	T(90),	P(10)	
1018	vw	1018	T(75),	P(24)	
		993	T(43),	β(31),	P(24)
990	w	988	β(50),	T(30),	P(16)
950	vw	962	T(54),	P(43)	
920	m, sh	932	P(51),	T(46)	
		902	P(58),	T(39)	
859	m	872	P(64),	T(33)	
832	m	842	P(69),	T(28)	
806	m	815	P(75),	T(23)	
782	m	787	P(79),	T(18)	
763	m	762	P(83),	T(14)	
749	w	739	P(87),	T(11)	
739	m	719	P(90)		
731	w, sh	702	P(93)		
		688	P(95)		
		677	P(97)		
		669	P(98)		
		663	P(99)		
716	s	660	P(100)		

the observed and calculated frequencies by a trial-and-error method. The calculated frequencies in the methylene progressive region from 700 to 1400 cm^{-1}, which were sensitive to the conformational change of the chain, are listed in Table 2—5 for n=14—20, respectively. The frequencies of the observed progressive bands were satisfactorily assigned according to the all-trans conformation, although the above-mentioned force constants gave slightly higher calculated frequencies for the CH_2 wagging modes.[7] The assignment was almost the same as that derived by Gotoh and Takenaka[8] for n=14 and 16, except for that of the CH_3 rocking band.

Second, the conformational change with an increase in the temperature was considered. With increasing temperature, the intensities of the progressive bands ascribed to the all-trans conformation decreased at the transition from phase I to II for n=16, as shown in Fig. 3. New bands appeared at 1348, 1077, 932, 867, 855, 772, and 752 cm^{-1} (marked with asterisks in Fig. 3). At the transition from phase II to III, the intensities of the progressive bands further decreased and those of the new bands observed in phase II decreased and became slightly detectable. At temperatures above phase IV, all of these bands were smeared out. Similar spectral changes were also observed for n=14, 18, and 20. The new bands observed in phases I′, II, and III for n=14—20 are summarized in Table 6.

Comparing the new bands observed in phases I′, II, and III with the conformationally disordered bands of normal alkanes, we considered the structural transition behavior. Because of the localized character of the defect modes in normal alkanes, they may be well transferable among the molecules of the same class, as in the present cases. The frequencies of the defect modes have been evaluated for the end gauche (*gt-* where *g* and *t* represented trans and gauche conformations, respectively, and the dash meant the remainder of the chain was in all-trans or nearly all-trans conformation), double gauche (*gg-*), and kink (*gtg′*) conformations by normal-mode analysis for normal alkanes.[9-11] According to the analysis, the new bands observed in phases I′, II, and III were assigned as listed in Table 6, indicating that there was a conformational defect at the methyl-end. With an increase in the chain length, there appeared *gtg′* conformation for n=20. There remained several bands which could not be assigned at the present stage. Based

Table 6. Frequencies (cm^{-1}) of Conformational Defect Bands Observed in Phases I′, II, and III for n=14—20

n=14	16	18	20	Assignment	Ref.
1348	1348	1348	1347	*gt-*	9
			1289	(*gtg′*)	10
1116				*	
			1095	(*gtg′*)	10
			1081	*	
1075	1077	1072	1075	*gt-*	9
943				*	
	932	928	933	(*gt-*)	10
	867			(*gt-*)	10
	855			*gg-*	11
770	772	774	776	*gt-*	10
			760	*	
748	752	754		*	

( ): uncertain. *: not assigned at the present stage.

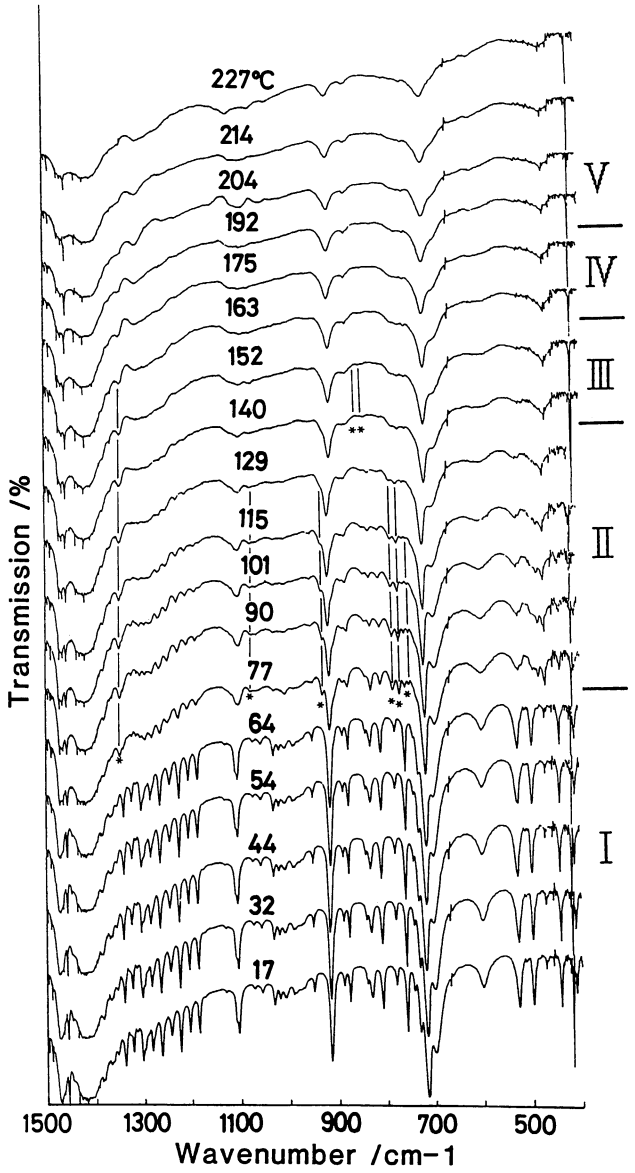

Fig. 3. Temperature dependence of IR spectrum for n=16 in the 400—1500 cm^{-1} region.

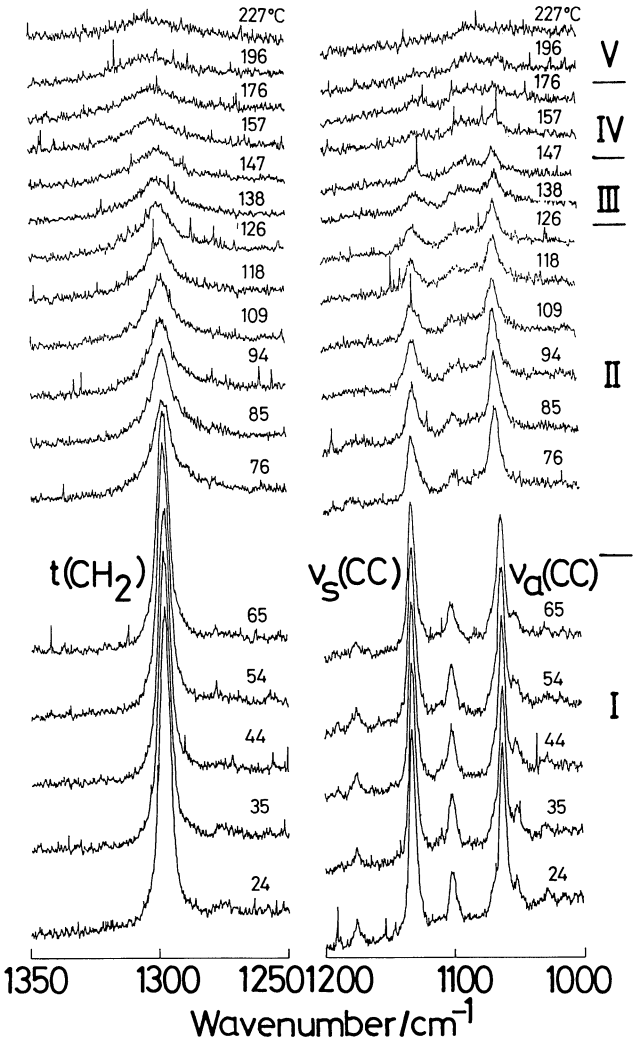

Fig. 4. Temperature dependence of Raman spectra for n=14.

on the result of a decrease in the intensities of the progressive bands and the appearance of defect bands, it was concluded that the conformational disordering proceeded in phases I′, II, and III, and the disappearance of these bands indicated that the chains went into a liquid state above phase IV for n=14—20.

In order to confirm the structural transition, the temperature dependence of the Raman spectra was observed, as shown in Fig. 4. The Raman spectra of the alkyl chains in the 1000—1500 cm^{-1} region are sensitive to the conformational order of the chains. The intensities of the bands at 1295 cm^{-1} [the CH_2 twisting $t(CH_2)$], and 1170 cm^{-1} [the CH_2 rocking $r(CH_2)$], as well as 1130, 1062 cm^{-1} [the symmetric and antisymmetric C–C stretchings ν_s(CC) and ν_a(CC)] are proportional to the amount of all-trans segments longer than a certain length characteristic of each vibrational mode. For example, the 1295 cm^{-1} band is due to all-trans sequences of 6 or more methylene units, the 1130 cm^{-1} band to those of 16—20 or more units, and the 1062 cm^{-1} band to those of 8 or more units.[12] The temperature dependence of the peak intensities of the Raman $t(CH_2)$, ν_s(CC), and ν_a(CC) modes relative to the peak intensity of the $t(CH_2)$ mode[13] at room temperature for n=14—20 is plotted in Fig, 5. With an increase in the temperature, at the transition from phase I to I′ or II, the intensity of the 1130 cm^{-1} band (which is characteristic of the long methylene sequences) decreased selectively. At the temperatures in phase II and III, the intensities of all of bands (including those characteristic of short trans sequences) decreased. At temperatures above phase IV, these bands were smeared out. Therefore, the result of the IR measurements was confirmed by the Raman measurements.

In conclusion, from the IR and Raman methods it was revealed for n=14—20 that the conformational disordering of the alkyl chains proceeded in phases I′, II,

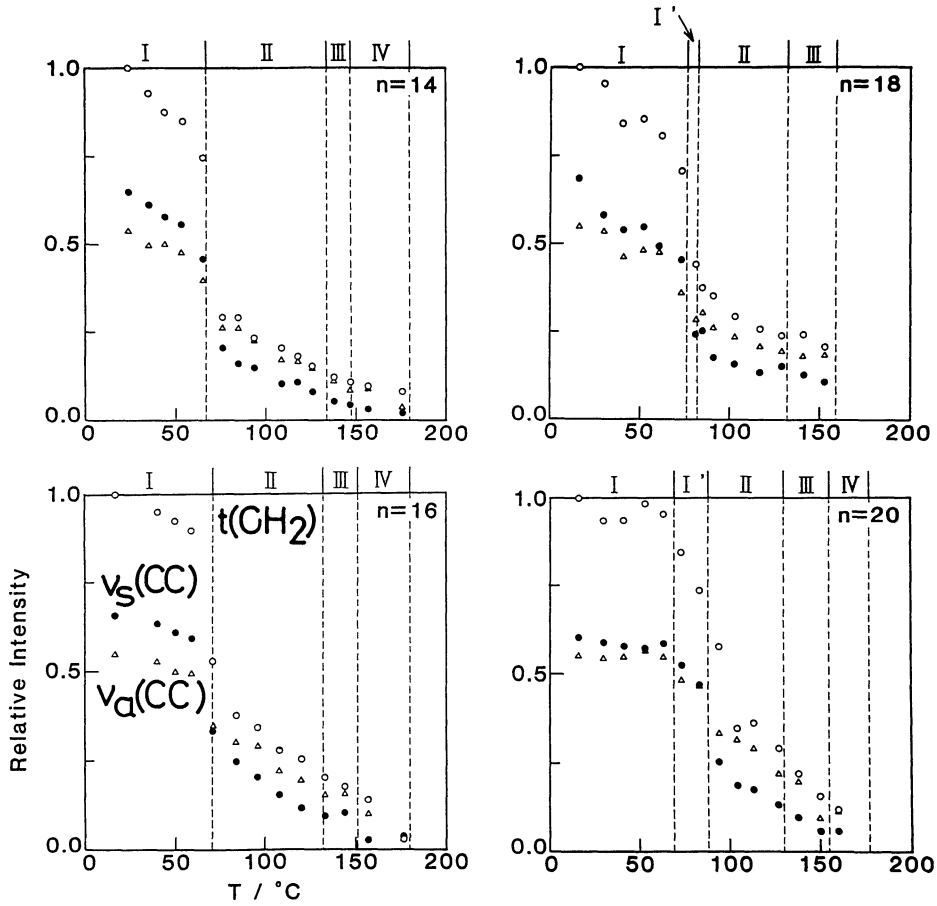

Fig. 5. Temperature dependence of relative peak intensities of Raman spectra for n=14—20.

and III. At temperatures above phase IV, the chains entered a liquid-like conformation.

References

1) D. M. Small, "Handbook of Lipid Research," Plenum Press, New York and London (1986), Vol. 4.
2) A. Cingolani, G. Spinolo, M. Sanesi, and P. Franzosini, *Z. Naturforsch., A,* **35**, 757 (1980).
3) K. Nakamura, *Nippon Kagaku Zasshi,* **79**, 1411 (1958).
4) J. H. Schachtschneider and R. G. Snyder, *Spectrochim. Acta,* **19**, 117 (1963).
5) J. Umemura, *J. Chem. Phys.,* **68**, 42 (1978).
6) T. Miyazawa, *Nippon Kagaku Zasshi,* **74**, 915 (1953).
7) R. G. Snyder, *J. Mol. Spectrosc.,* **23**, 224 (1967).
8) R. Gotoh and T. Takenaka, *Nippon Kagaku Zasshi,* **84**, 392 (1963).
9) M. Maroncelli, S. P. Qi, H. L. Strauss, and R. G. Snyder, *J. Am. Chem. Soc.,* **104**, 6237 (1982).
10) P. Jona, M. Gussoni, and G. Zerbi, *J. Appl. Phys.,* **57**, 834 (1985).
11) Y. Kim, H. L. Strauss, and R. G. Snyder, *J. Phys. Chem.,* **93**, 485 (1989).
12) M. Kobayashi, *J. Mol. Struct.,* **126**, 193 (1985).
13) G. R. Strobl and W. Hagedorn, *J. Polym. Sci., Polym. Phys. Ed.,* **16**, 1181 (1978).